

Development and *In Vitro* Evaluation of Nanoparticles of Silymarin Using Central Composite Design

Yashu Agrawal¹, Manoj Kumar Goyal²

¹SRNS Mahavidyalaya Pharmacy, Gormi, Gwalior (M.P.)

²Professor and HOD of Pharmaceutics, SRNS Mahavidyalaya Pharmacy, Gormi, Gwalior (M.P.)

Corresponding Author: Dr. Manoj Kumar Goyal

DOI: <https://doi.org/10.52403/ijrr.20231132>

ABSTRACT

Silymarin is a phytoconstituent derived from the plant *Silybum marianum* with poor oral absorption and bioavailability but possesses hepatoprotective activity, anticancer activity, cardioprotective, neuroprotective, stabilizing, anti-inflammatory, and antioxidant activity. Therefore, the current work aims to develop a nanoformulation of silymarin to increase bioavailability, reduce dosing frequency, minimize toxicity, and improve patient compliance. Silymarin nanoparticles were created via the ionic gelation technique, employing chitosan and TPP as the primary polymers. A central composite design was employed for formulation optimization. Chitosan and TPP were employed as independent variables, while particle size and encapsulation efficiency were considered as dependent variables. The prepared nanoparticles were evaluated through entrapment efficiency, *in vitro* drug release, and drug-excipient interaction studies. Thirteen experiments were conducted using the experimental runs created by the central composite design. The average particle size was between 149nm and 294nm. The encapsulation efficiency percentage was between 65.4% and 87.3%. The polydispersity index had a value of 0.437. The zeta potential of the optimized formulation was determined to be 38.1 mV. The compatibility studies between the drug and excipients were confirmed using Fourier Transform Infrared Spectroscopy and Differential Scanning Calorimetry. The successful encapsulation of silymarin within the polymer core was verified through scanning

electron microscopy analysis. The silymarin-loaded nanoparticles were observed to have a significant drug release of 98,942.43% over 24 hours. The outcomes of the study of Silymarin nanoparticles showed a substantial increase in the dissolution rate, which can be ascribed to the changed solubility properties of the drug. This result is consistent with the stated aim of improving drug absorption.

Keywords: Silymarin, nanoformulation, central composite design.

INTRODUCTION

Oral administration of medication is commonly employed to treat gastrointestinal disorders, whether they affect the entire body or are limited to the gastrointestinal tract. However, conventional oral dosage forms have several associated problems. These forms often require multiple daily administrations to maintain the drug concentration inside the therapeutically acceptable range. This leads to fluctuating drug levels, resulting in undesirable toxicity and reduced efficiency [1]. Controlled drug delivery systems have been devised to overcome the limitations associated with conventional oral dosage forms. The most significant hurdles in developing a controlled drug delivery system lie in regulating drug release and extending the dosage form's residence time at the absorption site, ensuring the complete drug release within the intended timeframe. The

goal of continuous drug release can be achieved by utilizing drug-carrying polymers that undergo gradual degradation over a specified period, thereby facilitating the controlled release of the drug [1].

Silymarin, a compound derived from *Silybum marianum* (L.) Gaertn, is classified as a flavonolignan. Silymarin has shown a range of pharmacological effects in many diseases. Silymarin is a complex of flavonolignans, including silybin, isosilybin, silydianin, and silychristine [2-5]. The substance exhibits low solubility in water and demonstrates hepatoprotective effects when administered orally at a dosage range of 240-800 mg/day, divided into two or three doses [6-7]. Oral administration results in peak plasma concentration within 2-4 hours, with a half-life of 6 hours. The limited bioavailability of the compound is primarily attributed to its extensive metabolism, low solubility in water, rapid elimination through urine and bile, and low ability to cross intestinal epithelial cells. The given text represents a numerical range from 8 to 9. The limited duration of action, low absorption rate, and frequent dosing requirements of silymarin have created significant opportunities to advance nanoparticle-based drug delivery systems [8-9].

Nanotechnology has shown its ability to overcome the divide between the medical and physical sciences by utilizing nanostructures and nanophases across several scientific disciplines. This is particularly evident in nanomedicine and nano-based drug delivery systems, where the investigation and use of such particles have garnered significant attention. Furthermore, it has been observed that nanostructures play a crucial role in avoiding the degradation of pharmaceuticals inside the gastrointestinal tract and facilitate the targeted transport of medications with limited solubility in water to their intended site of action. Nano drugs demonstrate increased oral bioavailability due to their capacity to engage in absorptive endocytosis, a common cellular absorption

method. Nanostructures exhibit an extended residence time inside the bloodstream, enabling the controlled release of combined pharmaceutical agents at predetermined dosages. Nanoparticles have been seen to induce fewer plasma fluctuations, and exhibit diminished deleterious effects. Consequently, they have demonstrated use in information acquisition, as evidenced by their application in many innovative assays for disease treatment and diagnosis [10-11]. To address this issue, it is advisable to employ a design of experiment methodology, such as the Central Composite Design (CCD), within the Response Surface Methodology (RSM) framework. By incorporating these techniques into the design and development process, it becomes possible to effectively assess the combined impact of various variables on the outcomes and quality of products. Furthermore, Central Composite Design (CCD) has proven to be efficacious in numerous research endeavors to formulate and refine various substances. The data from CCD has consistently demonstrated its capacity to yield accurate and dependable predictions [12].

Chitosan is a naturally occurring polysaccharide derived from various sources such as Crustaceans, insects, and fungi. It possesses several notable properties, including gelation, film-forming ability, and bioadhesiveness characteristics, and acts as a penetration enhancer [13]. It exerts a beneficial impact on the opening of tight junctions in epithelial cells. Due to its inherent polymeric cationic characteristics, this substance can interact with molecules and polymers with a negative charge. The synthesis of chitosan nanoparticles was achieved by exploiting the ionic interaction between cationic chitosan and anionic counter ions, specifically tripolyphosphate. This interaction led to the formation of polymer linkages [13-15]. The degradation of chitosan is subject to the influence exerted by its molecular weight and degree of deacetylation. The molecular weight of a substance exerts a significant impact on its

absorption and distribution within an organism. It has been observed that substances possessing greater molecular weights exhibit a propensity for accelerated excretion, thereby minimizing their absorption into the system [15].

This research aimed to create a Silymarin controlled-release formulation that would stay in the absorption site over the drug's half-life. The objective of this formulation was to improve the bioavailability of the drug, reduce the frequency of dosing, minimize potential toxicity, and enhance patient compliance.

MATERIAL AND METHOD

Silymarin was purchased from Yarrow Chem Products. Chitosan (CH) (deacetylation 93%, MW 161.16 (kDa), and Sodium Tripolyphosphate (TPP) were procured from CDH Fine Chemical, India. All other reagents and solvents used were of analytical grade.

Preparation of silymarin-chitosan nanoparticles

Nanoparticles were devised using the ionotropic gelation method, as described by Nagpal et al. and Chuah et al. A 2% aqueous solution of acetic acid was used to prepare various concentrations of chitosan solution. The pH of the mixture was successfully maintained using 1M sodium hydroxide solution. 10 mg of silymarin was dissolved in 1 mL of ethanol to create a drug solution. After that, the resultant solution was carefully and gradually added to the CH solution while stirring constantly for 45 minutes using a magnetic stirrer. Various concentrations of sodium TPP solution were prepared following the experimental requirements, and their pH was adjusted to 5 using a 0.1M HCl solution. TPP solution was added drop by

drop to the chitosan solution under continuous stirring for 1 hour at 800 rpm. The produced nanoparticles were separated using centrifugation at 16,000 rpm at a temperature of 30°C for 15 minutes. The pellet produced after centrifugation was reconstituted in 10 mL of distilled water and subsequently subjected to sonication for 30 minutes using a bath sonicator. The prepared nanoparticles were lyophilized after including 5% D-mannitol as a cryoprotectant. Following that, the nanoparticles were promptly subjected to freeze-drying to avoid any potential particle aggregation.

Experimental design

The concentration of CH (X1) and the ratio of TPP (X2) were identified as independent factors that had a statistically significant influence on both the particle size (Y1) and entrapment efficiency (Y2). These conclusions were drawn based on the findings obtained during the preliminary tests. Hence, a central composite experimental design was used to improve the formulation of chitosan nanoparticles loaded with silymarin. This design had a 2-factor 3-level (3)² configuration, which encompassed both negative ($-\alpha$) and positive ($+\alpha$) values. The experimental design, which includes the formulation parameters, has been outlined in Table 1. The test variables were given numerical codes of -1, 0, and +1 to indicate distinct amounts of CH (30, 40, and 50 mg) and TPP ratios (3:1, 3.6, and 4:1). Preliminary experiments were undertaken to ascertain the optimal values of the independent variables. The experimental results indicated that changing the CH amount within the range of 30 to 50 mg and varying the TPP ratio from 3:1 to 4:1 substantially affected the formation of the nanoparticles.

Table 1. Coded value with central composite design.

Factors	Low value	Mid value	High value	- α	+ α
A: Chitosan	30	40	50	25.8579	54.1421
B: TPP	3.1	3.6	4.1	2.89289	4.30711

Characterization

Determination of particle size and size distribution

The dynamic light scattering method was used to determine the particle size and polydispersity index (PDI) of the nanoparticles. The ZetaSizer Nano ZS90 was used for this specific purpose. In order to determine the particle size and PDI, a 10-fold dilution of the sonicated dispersion containing 1 mL of the material was performed using double distilled water [18].

Determination of encapsulation efficiency

The nanoparticle suspension underwent centrifugation at 16,000 rpm for 15 minutes at a temperature of 10°C. The procedure was conducted via a chilling centrifuge. The liquid portion produced after the centrifugation was diluted by a factor of 10 using double distilled water to ascertain the concentration of unbound silymarin. The accomplishment was attained using a UV-visible spectrophotometer to measure the absorbance of the diluted solution at a wavelength of maximum absorption (λ_{max}) of 287 nm. The calculation of encapsulation efficiency for nanoparticles was performed using the following equation [19].

Drug content

Drug content was quantified by extracting a volume of 1 ml from the chitosan nanoparticles. The prepared nanoparticle samples (1ml) were subjected to adding 1ml of aqueous potassium dihydrogen phosphate. The resulting mixture was then centrifuged at 16000 revolutions per minute at a temperature of 30°C. The transparent liquid portion was extracted and subjected to analysis using a spectrophotometric technique, allowing for the determination of the drug content. The samples underwent triplicate examination, while the resultant data was presented as the mean value \pm standard deviation [20].

Scanning Electron microscopy

The investigation of the uniformity in the particle's shape and the structure of the

produced nanoparticles was carried out using scanning electron microscope. The dispersion of nanoparticles in water was successfully accomplished, and afterwards, they were applied onto an aluminium stub using a double-sided carbon tape through the drop coating technique. The sample underwent a gold sputter coating process using the SC7620 equipment, with a vacuum pressure of 10 Pa maintained for a period of 10 seconds. The image was successfully magnified to the appropriate level by employing a standard acceleration potential of 30 kilovolts [21].

In-vitro drug release study

In-vitro release study was carried out using the USP XXII dissolution apparatus II, (paddle-type). Nanoparticles containing a pharmaceutical dose of 5 mg were encapsulated within a dialysis membrane bag manufactured by Himedia. The dialysis membrane exhibits a molecular weight cutoff range of 12,000-14,000 and a pore size of 2.4 nm. The membrane bag was then placed in a flask with 250 ml of phosphate buffer solution (pH 7.4) and 0.1% tween 20. Tween 20 has been used as a component in dissolution media for pharmaceuticals exhibiting limited solubility. The paddle underwent rotation at a rate of 50 rpm. The solvent temperature was maintained at a constant value of 37°C \pm 1°C. A 5 ml sample was collected from the solution at specific time intervals (0.25, 0.50, 1, 2, 3, 4, 5, 6, 8, 9, 11, and 24 hours) and replaced with fresh dissolving medium. The samples were analyzed using a UV spectrophotometer to measure absorbance at a wavelength of 287 nm. The dissolution tests were performed in triplicate [22].

Drug Excipient Compatibility Studies

Differential Scanning Calorimetry

The experimental investigation used the DSC-60, a differential scanning calorimeter produced by Shimadzu in Japan. The samples were examined within a temperature range from 0 °C to 400 °C, with a heating rate of 5 °C per minute, under a

protective nitrogen environment. The specimens underwent preparation by compression inside a specially built aluminium pan for differential scanning calorimetry, followed by subsequent analysis. The current study investigated possible physical interactions between the medication and any existing polymers.

FT-IR Spectroscopy

The FTIR spectra were acquired utilizing the Perkin-Elmer Life and Analytical Sciences instrument. The samples are prepared by mixing them with potassium bromide (KBR) and subsequently pressed into a disc. These discs are then analyzed using an infrared (IR) beam, which scans the samples within the 400 to 4000 cm⁻¹ range. Spectral graphs were acquired for the pure drug, pure polymer, and formulated nanoparticles. This study successfully confirmed the authenticity of the starting materials while determining any chemical interactions between the drug and excipients, if present.

STATISTICAL ANALYSIS

Identifying the most suitable and varying amount of the independent variables, specifically chitosan and TPP, of the developed formulation was shown to depend on the responses' conditions in achieving the minimum particle size and maximum encapsulation efficiency. Examining the Y-response function's reaction patterns entailed applying the extended response surface model and polynomial Equation (1).

$$Y = \beta_0 + \beta_1x_1 + \beta_2x_2 + \beta_{11}x_1^2 + \beta_{22}x_2^2 + \beta_{12}x_1x_2(3)$$

The analysis of variance is a statistical method employed to investigate and assess the variations among multiple factors. In the simplified model, it was observed that all variable effects were deemed insignificant, as indicated by p-values greater than 0.05. The interaction effects between the factors and their corresponding responses were depicted through three-dimensional response plots.

RESULTS AND DISCUSSION

Data analyses and validation of optimization model for nanoparticles

The formulation optimization of NPs using response surface methodology (RSM) was conducted using Design Expert version 13.0.5.0, developed by Stat Ease, Inc. The objective of the optimization process was to enhance the entrapment efficiency and attain a particle size of around 100 nm. This was accomplished by altering the ratio of CH and TPP in the formulation being created. The quadratic model was chosen to represent the relationship between encapsulation effectiveness and the particle size, while the linear model was picked for the particle size. Multiple linear regression studies were conducted to obtain a polynomial equation. The statistical analysis revealed that the model had a significant effect (P < 0.05), whereas the lack of fit was determined to be non-significant (P > 0.05). The response variables, particle size (Y1), and entrapment efficiency (Y2) were best fitted by the quadratic or linear models without any adjustment.

Table 2. Recommended design through DOE for silymarin nanoparticles

Std	Run	Space Type	Factor 1 A: Chitosan Mg	Factor 2 B: TPP mg	Response 1 PS nm	Response 2 EE %
7	1	Axial	40	2.89289	120.65	69.02
4	2	Factorial	50	4.1	118.3	74.52
10	3	Center	40	3.6	103.45	73.36
13	4	Center	40	3.6	108.45	81.65
3	5	Factorial	30	4.1	78.63	70.68
5	6	Axial	25.8579	3.6	72.8	69.82
6	7	Axial	54.1421	3.6	115.5	68.82
11	8	Center	40	3.6	112.76	77.95
8	9	Axial	40	4.30711	85.35	83.71
1	10	Factorial	30	3.1	93.41	53.69
2	11	Factorial	50	3.1	128.2	64.85

9	12	Center	40	3.6	102.7	79.23
12	13	Center	40	3.6	105.26	72.92

Response surface analyses

The 3D-response surface graphs shown in Figures 10 and 11 were developed using Design Expert software in a three-dimensional format. Upon analyzing the three-dimensional curve shown in Figure 10, a distinct correlation between EE and the TPP ratio becomes evident. In particular, as the ratio transitions from 3:1 to 4:1, the variable EE exhibits a linear relationship, displaying a consistent and incremental growth. Conversely, a non-linear connection exists between the concentration of EE and CH. At the outset, the variable EE undergoes a rise, culminating in its peak magnitude.

However, additional increases in CH concentration lead to a subsequent decrease in EE. The observed behavior may be ascribed to the optimum rigidification of

nanoparticles within the intermediate CH content range, precisely at 40.0 mg. Upon examination of the three-dimensional response curve displayed in Figure 11, it is evident that a negative correlation exists between particle size and TPP, whereas a positive correlation is seen between particle size and CH concentration. The smallest particle size is possible when the concentration of middle CH and the TPP ratio are both at intermediate levels.

Table 9 displays the criteria for optimizing silymarin nanoparticles, including aims, limitations, and significance. The parameters for achieving an optimized nanoparticle solution were established to attain maximum entrapment efficiency while aiming for a particle size of around 100 nm. The desirability and overlay plot are shown in Figures 12 and 13.

Table no 3. Summary of suggested model of ANOVA for all responses.

Source	Sum of Squares	Df	Mean Square	F-value	p-value	
For response 1						
Model	3442.78	5	688.56	26.51	0.0002	significant
A-Chitosan	2670.37	1	2670.37	102.80	< 0.0001	
B-TPP	695.68	1	695.68	26.78	0.0013	
AB	5.95	1	5.95	0.2292	0.6467	
A ²	69.99	1	69.99	2.69	0.1447	
B ²	3.88	1	3.88	0.1494	0.7106	
Residual	181.83	7	25.98			
Lack of Fit	113.56	3	37.85	2.22	0.2285	not significant
Pure Error	68.27	4	17.07			
Cor Total	3624.61	12				
For Response 2						
Model	546.64	5	109.33	4.01	0.0489	significant
A-Chitosan	23.07	1	23.07	0.8463	0.3882	
B-TPP	281.26	1	281.26	10.32	0.0148	
AB	13.40	1	13.40	0.4914	0.5059	
A ²	216.44	1	216.44	7.94	0.0259	
B ²	29.39	1	29.39	1.08	0.3337	
Residual	190.83	7	27.26			
Lack of Fit	133.43	3	44.48	3.10	0.1515	not significant
Pure Error	57.39	4	14.35			
Cor Total	737.46	12				

Table No. 4: - Appropriate model suggested for PS and EE.

Responses	Std. Dev.	Mean	C.V. %	R ²	Adjusted R ²	Predicted R ²	Adeq Precision
R1	5.10	104.11	4.90	0.9498	0.9140	0.7478	15.9396
R2	5.22	72.32	7.22	0.7412	0.5564	-0.4083	6.0233

Table No. 5: Fit statistics for selected models for Particles Size and Entrapment efficiency.

Response 1					
Source	Sequential p-value	Lack of Fit p-value	Adjusted R ²	Predicted R ²	
Linear	< 0.0001	0.2856	0.9144	0.8703	Suggested
2FI	0.6560	0.2377	0.9071	0.8353	
Quadratic	0.3164	0.2285	0.9140	0.7478	
Cubic	0.2313	0.2369	0.9330	0.3885	Aliased

Response II					
Linear	0.0699	0.0877	0.2952	-0.0613	
2FI	0.6050	0.0709	0.2411	-0.8567	
Quadratic	0.0634	0.1515	0.5564	-0.4083	Suggested
Cubic	0.5739	0.0614	0.5027	-7.4031	Aliased

Particle size and of nanoparticles

The particle size of the samples, produced according to the experimental design and the final optimized batch, is shown in Table 9. The particle size of the nanoparticles exhibited a range of 72.8 nm to 135.3 nm.

Entrapment efficiency of nanoparticles

The drug encapsulation efficiency of the produced nanoparticles was within the range -[
0

of 69.82% - 83.71%. However, the EE was determined to be 69.82 % for the optimized batch. The study revealed that the entrapment efficiency has an upward trend as the TPP ratio increases. Additionally, it was shown that the entrapment efficiency first rises and then declines when the concentration of CH increases within the range of 30.0 to 50.0.

Figure 1. Response surface plot for particle size.

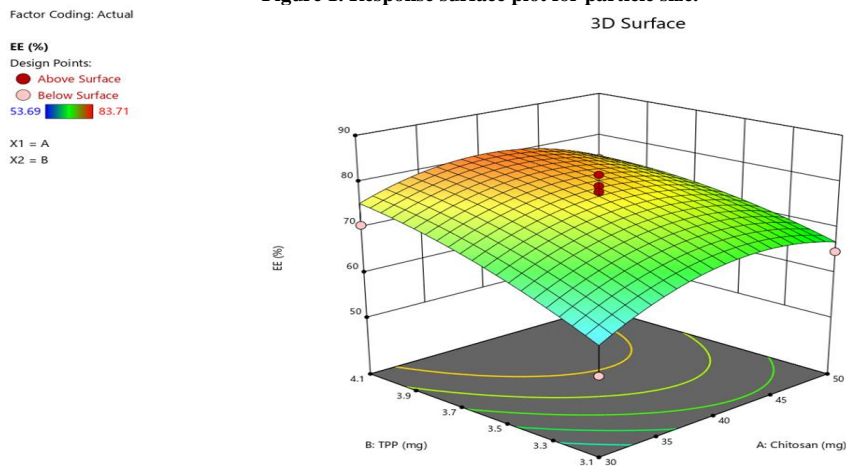


Figure 2. Response surface plot for percentage encapsulation efficacy.

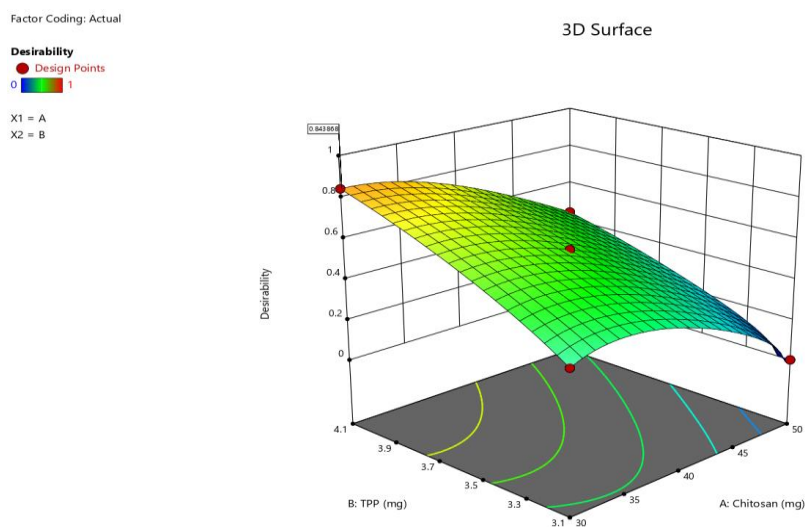


Figure 3. Response surface plot for the overall desirability function.

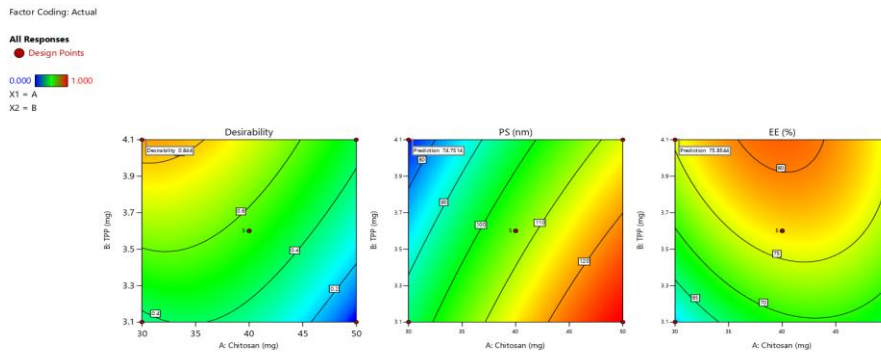


Figure 4. Contour plot of optimized formulation.

In vitro drug release Optimized formulation

The release profiles of chitosan nanoparticles containing silymarin from various formulations (F1 - F13) were evaluated in phosphate buffer with a pH of

7.4 over 24 hours (Table 16). The maximum drug release was seen in formulation F6 compared to the other formulations. The percentage of cumulative drug release (% CDR) for the F6 formulation was 89.96% (Figure 5).

Table 6. In vitro release data of various formulations.

Time	F1	F2	F3	F4	F5	F6	F7	F8	F9	F10	F11	F12	F13
0	0	0	0	0	0	0	0	0	0	0	0	0	0
1	7.87 717	7.52 99	7.4141 5	6.6617 4	7.64 566	6.95 113	5.7935 7	6.2565 9	6.14 084	9.0630 9	8.6919 6	9.43 423	8.02 392
2	14.2 875	14.7 486	17.063 1	14.628	15.2 123	12.3 145	13.465 6	13.931	12.8 309	20.544 4	15.494 9	25.3 712	17.4 953
3	20.2 702	21.4 284	26.765 3	22.406 8	19.5 795	20.7 171	19.559 5	20.490 7	17.8 216	28.155 1	22.261 1	33.9 737	28.9 489
4	26.4 014	29.8 811	36.521	32.312	25.4 753	26.8 509	26.265 7	25.118 4	22.8 396	42.042 6	34.854 1	45.6 665	43.2 121
6	34.1 866	35.4 863	46.33	38.972 5	32.3 294	32.3 236	29.998 8	37.526 8	32.8 046	51.627 6	44.398 9	56.3 841	53.3 969
8	48.6 124	44.4 786	56.192 4	46.537 1	39.2 207	37.4 786	37.629 7	50.582 2	39.6 41	63.341 6	52.511 1	63.3 607	61.7 07
16	57.3 295	55.6 613	67.207 9	55.589 6	55.8 729	55.8 574	60.118 8	61.509 5	58.6 687	73.635 3	71.281 5	71.5 887	68.5 029
24	84.0 356	85.7 729	83.954 9	80.317 9	84.1 919	89.9 642	84.641 7	82.508 9	87.0 613	92.297 6	87.111 2	88.1 607	89.7 347

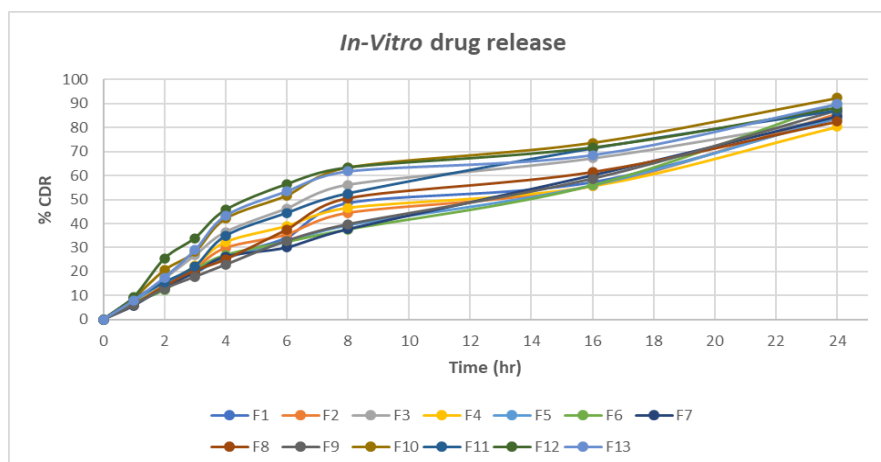


Figure 5. In-vitro drug release for F1-F13.

Kinetic models

Various kinetic models, including the zero-order, first-order, Higuchi's square model, and Korsmeyer Peppas model, were used to analyze the release behavior of Silymarin from diverse formulations. The optimized formulation F6, which follows Kros-Peppas

order kinetics, exhibits a correlation coefficient (r^2) 0.9733. In comparison, the first-order model yields a correlation coefficient of 0.9704. Therefore, the drug release mechanism of formulation F6 may be classified as Fickian release (Figure 6).

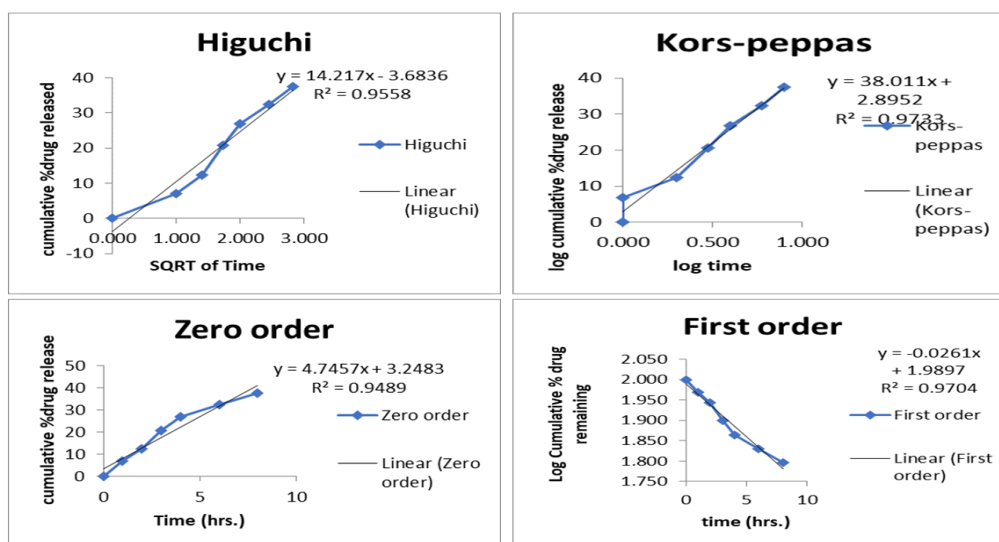


Figure 9. Suggested kinetic release model for silymarin nanoparticles from A-D.

SEM

The surface structure and morphology of the optimized formulation, F7, are shown in Figure 10. The photomicrograph of the nanoparticle was rough in shape.

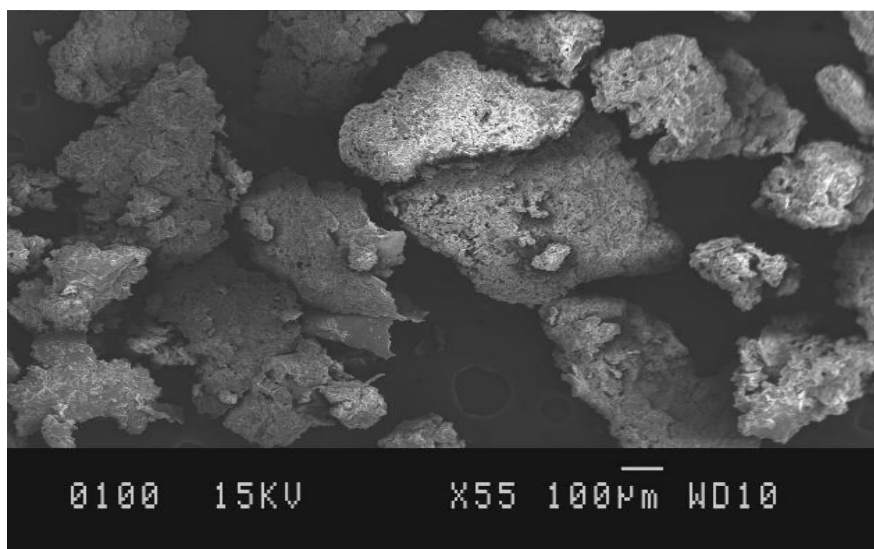


Figure 7. This shows the SEM image of optimized formulation.

Differential Scanning Calorimetry

Differential scanning calorimetry (DSC) is a technique used to quantify the thermal energy exchange, either in the form of heat loss or gain, due to physical or chemical

transformations inside a given sample to temperature. A distinct and symmetrical endothermic melting peak may serve as an indicator of relative purity, whereas a broader and asymmetric curve may reveal

the presence of impurities or several thermal processes. Differential scanning calorimetry (DSC) study was conducted to determine Silymarin's physical characteristics.

Thermograms of the pure drug, polymer, and physical combination were obtained using individual DSC analyses. These thermograms are shown in Figure 8.

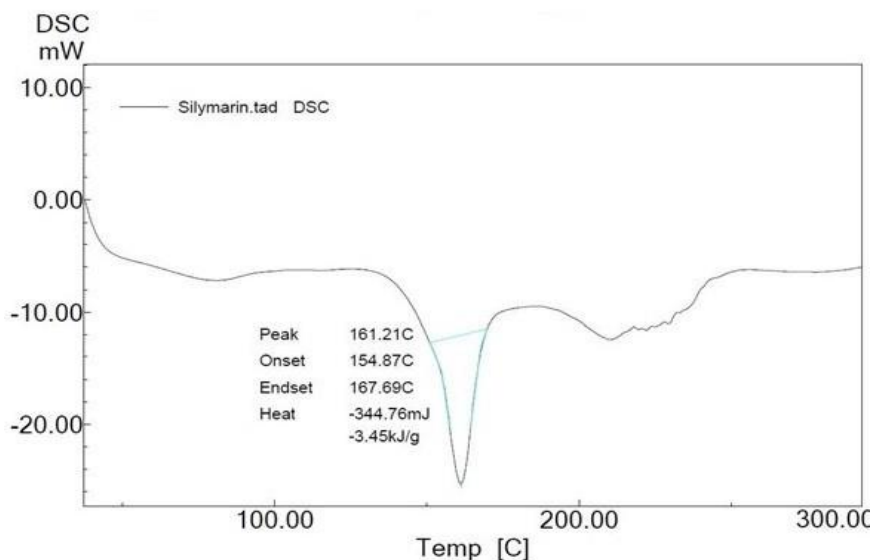


Figure 8. DSC thermogram of Silymarin

DISCUSSION

The current study aimed to enhance the solubility and bioavailability of silymarin by developing a nanoformulation. Additionally, the study aimed to regulate the release of silymarin from the dosage form to obtain an extended period of action.

The spectra obtained from the sample drug were compared to those of the standard pure medication using FTIR and UV spectral examinations, confirming their authenticity. The UV spectra exhibited a prominent absorption peak at a wavelength of 288nm. The analysis of FTIR spectra for both silymarin and a mixture of silymarin and polymer indicates that no new peaks are observed, and no existing peaks are lost compared to the spectra of the medication alone. This finding suggests a lack of interaction between the medicine and polymer employed in the investigation.

The ionic gelation process was employed to synthesize Chitosan and TPP Nanoparticles. The employed approach demonstrated simplicity and cost-effectiveness. The entrapment efficiency of formulations F1 - F13 ranges from 68.82% to 83.71%, while the particle size ranges from 72.8 nm to

120.65 nm. These measurements are considered for the determination of Zeta potential and SEM examination.

The scanning electron micrograph of the chitosan nanoparticle preparation revealed that the nanoparticles exhibited a polydispersed spherical morphology. The SEM pictures provided unequivocal evidence of the spherical shape and polydispersity of the chitosan nanoparticles. The determination of particle size and zeta potential was conducted using the Malvern Zeta sizer. The particle size examination confirmed that the processed sample exhibited dimensions within the nanoscale scale. The average particle size obtained for formulation F6 was 72.8 nm. The observed zeta potential values suggest the stability of the formed chitosan nanoparticle.

Based on the *in-vitro* release data obtained by the dialysis bag diffusion method, it was observed that formulations F1 to F13 exhibited drug release percentages ranging from 80.03% to 89.96% over 24 hours. The drug release data from *in-vitro* experiments demonstrates that the hydrophobic polymer chitosan and TPP exhibit a sustained drug release profile. The observation of drug

release was found to be dependent on the ratio of drug to polymer. Both the quantities of Chitosan and TPP demonstrated a noteworthy influence on the release of the medication. The experimental findings indicate that a lower concentration of chitosan and a medium-range concentration of TPP resulted in a higher amount of drug release. This phenomenon can be attributed to the delayed drug release, which arises from the hindered diffusion of the drug inside the polymer matrix that has experienced more significant swelling due to higher concentration.

The data acquired from the *in vitro* release investigation was subjected to fitting with models to determine the mechanism of drug release from silymarin chitosan nanoparticles. The Kros-Peppas release order was the most suitable *in vitro* release model. The confirmation of this was achieved through the charting of the percentage cumulative drug release against the logarithm of time. The resulting r^2 values ranged from 0.903 to 0.9733.

CONCLUSION

The optimization process for chitosan nanoparticles was effectively performed in creating an appropriate drug carrier for the oral administration of silymarin. The data obtained from the study indicate that the formulations of chitosan nanoparticles, which were optimized using the central composite design (CCD) approach, were found to be suitable and reliable. The comprehension of the correlation between chitosan and TPP, which serve as the primary constituents of polymeric nanoparticle formulation, and their influence on the particle size and encapsulation efficacy has been effectively elucidated through the response surface plots generated within the scope of this investigation. Hence, the chitosan nanoparticles' optimized compositions, as proposed by the response surface methodology (RSM), were deemed satisfactory. The assessment of drug release percentage revealed a favorable release

profile for silymarin. Based on the findings of this *in vitro* drug release study, it can be inferred that using chitosan nanoparticles effectively extends the duration of silymarin release and improves its relative oral bioavailability.

Declaration by Authors

Ethical Approval: Approved

Acknowledgement: The authors are thankful to the SRNS Mahavidyalaya Pharmacy, Gormi, Gwalior (M.P.), India for providing the necessary facilities for my research work.

Source of Funding: None

Conflict of Interest: The authors declare no conflict of interest.

REFERENCE

1. Yie WC. Concepts and System Design for Rate-controlled Drug Delivery. Novel Drug Delivery System, 2nd ed.; Marcel Dekker: New York, p. 1-42; 1992.
2. Flora K, Hahn M, Rosen H, Benner K. Milk thistle (*Silybum marianum*) for the therapy of liver disease. *Am J Gastroenterol* 1998; 93:139-43.
3. Negi AS, Kumar JK, Luqman S, Shanker K, Gupta MM, Khanuja SP. Recent advances in plant hepatoprotectives: A chemical and biological profile of some important leads. *Med Res Rev* 2008; 28:746-72.
4. Pei YP, Chen J, Li WL. Progress in research and application of silymarin. *Med Aromat Plant Sci Biotechnol* 2009; 3:1-8.
5. Mourelle M, Muriel P, Favari L, Franco T. Prevention of CCL4-induced liver cirrhosis by silymarin. *Fundam Clin Pharmacol* 1989; 3:183-91.
6. Ding T, Tian S, Zhang Z, Gu D, Chen Y, Shi Y, et al. Determination of active component in silymarin by RP-LC and LC/MS. *J Pharm Biomed Anal* 2001; 26:155-61.
7. Kvasnicka F, Bíba B, Sevcík R, Voldrich M, Krátká J. Analysis of the active components of silymarin. *J Chromatogr A* 2003; 990:239-45.
8. Wagner H, Seligmann O. Liver therapeutic drugs from *Silybum marianum*. In: Chang HM, Yeung HW, Tso WW, Koo A, editors. *Advances in Chinese Medicinal Materials*

- Research. Singapore: *World Scientific Publ. Co.*; 1985.
- Javed S, Kohli K, Ali M. Reassessing bioavailability of silymarin. *Altern Med Rev* 2011;16:239-49.
 - Patra JK, Das G, Fraceto LF, Campos EVR, Rodriguez-Torres MDP, Acosta-Torres LS, Diaz-Torres LA, Grillo R, Swamy MK, Sharma S, Habtemariam S, Shin HS. Nano based drug delivery systems: recent developments and future prospects. *J Nanobiotechnology*. 2018 Sep 19;16(1):71. doi: 10.1186/s12951-018-0392-8. PMID: 30231877; PMCID: PMC6145203.
 - Salata O. Applications of nanoparticles in biology and medicine. *J Nanobiotechnology*. 2004 Apr 30;2(1):3. doi: 10.1186/1477-3155-2-3. PMID: 15119954; PMCID: PMC419715.
 - Asadollahzadeh M, Tavakoli H, Torab-Mostaedi M, Hosseini G, Hemmati A. Response surface methodology based on central composite design as a chemometric tool for optimization of dispersive-solidification liquid-liquid microextraction for speciation of inorganic arsenic in environmental water samples. *Talanta*. 2014 Jun; 123:25-31. doi: 10.1016/j.talanta.2013.11.071. Epub 2014 Feb 8. PMID: 24725860.
 - Casadidio C, Peregrina DV, Gigliobianco MR, Deng S, Censi R, Di Martino P. Chitin and Chitosans: Characteristics, Eco-Friendly Processes, and Applications in Cosmetic Science. *Mar Drugs*. 2019 Jun 21;17(6):369. doi: 10.3390/md17060369. PMID: 31234361; PMCID: PMC6627199.
 - Cheung RC, Ng TB, Wong JH, Chan WY. Chitosan: An Update on Potential Biomedical and Pharmaceutical Applications. *Mar Drugs*. 2015 Aug 14;13(8):5156-86. doi: 10.3390/md13085156. PMID: 26287217; PMCID: PMC4557018.
 - Guan J (2011) Optimized Preparation of Levofloxacin-loaded Chitosan Nanoparticles by Ionotropic Gelation. *Int. Conf. on Phy. Sci. and Tech* 22: 163-169.
 - Chuah LH, Billa N, Roberts CJ, Burley JC, Manickam S. Curcumin-containing chitosan nanoparticles as a potential mucoadhesive delivery system to the colon. *Pharm Dev Technol* 2013; 18:591-9.
 - Nagpal K, Singh SK, Mishra DN. Optimization of brain targeted gallic acid nanoparticles for improved antianxiety-like activity. *Int J Biol Macromol* 2013; 57:83-91.
 - Yan W, Fan W, Xu Z, Ni H (2012) Formation mechanism of monodisperse, low molecular weight chitosan nanoparticles by ionic gelation technique. *colloids and surfaces B: Biointerfaces* 90: 21-27.
 - Deshmukh, R., Harwansh, R. K., Prajapati, M., & Sharma, B. (2023). Formulation and Evaluation of Oral Mucoadhesive Microspheres of Ofloxacin for Peptic Ulcer Use. *Trends in Sciences*, 20(9), 5751. <https://doi.org/10.48048/tis.2023.5751>.
 - Mahendra Prajapati, Shradha Shende, Vivek Jain, Akhil Gupta, Manoj Kumar Goyal. Formulation and In vitro Percutaneous Permeation and Skin accumulation of Voriconazole Microemulsified Hydrogel. *Asian Journal of Pharmacy and Technology*. 2021; 11(4):267-2. doi: 10.52711/2231-5713.2021.00044.
 - Gupta S, Singh SK, Girotra P. Targeting silymarin for improved hepatoprotective activity through chitosan nanoparticles. *Int J Pharm Investig*. 2014 Oct;4(4):156-63. doi: 10.4103/2230-973X.143113. PMID: 25426436; PMCID: PMC4241620.
 - Weng J, Tong HHY, Chow SF. In Vitro Release Study of the Polymeric Drug Nanoparticles: Development and Validation of a Novel Method. *Pharmaceutics*. 2020 Aug 4;12(8):732. doi: 10.3390/pharmaceutics12080732. PMID: 32759786; PMCID: PMC7465254.

How to cite this article: Yashu Agrawal, Manoj Kumar Goyal. Development and in vitro evaluation of nanoparticles of silymarin using central composite design. *International Journal of Research and Review*. 2023; 10(11): 269-280. DOI: <https://doi.org/10.52403/ijrr.20231132>
